Developmental Biology 373 (2013) 184–195

Contents lists available at SciVerse ScienceDirect

Developmental Biology

journal homepage: www.elsevier.com/locate/developmentalbiology

The contactin RIG-6 mediates neuronal and non-neuronal cell migration in *Caenorhabditis elegans*

Markella Katidou [a,b], Nektarios Tavernarakis [a,**], Domna Karagogeos [a,b,*]

[a] Institute of Molecular Biology and Biotechnology, Foundation for Research and Technology-Hellas, Heraklion, Crete, Greece
[b] University of Crete, School of Medicine, Department of Basic Sciences, Heraklion, Greece

ARTICLE INFO

Article history:
Received 18 January 2012
Received in revised form
22 October 2012
Accepted 25 October 2012
Available online 1 November 2012

Keywords:
Axon navigation
Axon outgrowth
Branching
Tubulogenesis

ABSTRACT

Cell adhesion molecules of the Immunoglobulin Superfamily (IgCAMs) are key factors in nervous system formation. The contactin subgroup of IgCAMs consists of GPI-anchored glycoproteins implicated in axon outgrowth, guidance, fasciculation and neuronal differentiation. The mechanism by which contactins facilitate neuronal development is not understood. To gain insight into the function of contactins, we characterized RIG-6, the sole contactin of *Caenorhabditis elegans*. We show that the contactin RIG-6 is involved in excretory cell (EC) tubular elongation. We also show that RIG-6 mediates axon outgrowth and guidance along both the anterior–posterior and dorso-ventral axis, during *C. elegans* development. We find that optimal RIG-6 expression is critical for accurate mechanosensory neuron axon elongation and ventral nerve cord architecture. In addition, our data suggest that the cytoplasmic UNC-53/NAV2 proteins may contribute to relay signaling via contactins.

Introduction

Many families of extracellular molecules and their receptors, including the Immunoglobulin Superfamily Cell Adhesion Molecules (IgCAMs), actively participate in cell interactions and signal transduction (Rougon and Hobert, 2003). IgCAMs have been shown to play vital roles in nervous system development and function: they are involved in axon outgrowth, fasciculation, migration and synaptic targeting (Brummendorf and Rathjen, 1996; Kolodkin and Tessier-Lavigne; Maness and Schachner, 2007). Deficiencies in these molecules are correlated with severe neurological disorders, highlighting the significance of their function (Katidou et al., 2008; Maness and Schachner, 2007).

IgCAMs are conserved among such diverse species as *Caenorhabditis elegans* and mammals (Hutter et al., 2000). The nematode has been instrumental in deciphering IgCAM involvement in nervous system development. UNC-40 and UNC-5, the receptors of UNC-6/netrin, which was first identified in worms, and SAX-3, the receptor of slit, in parallel direct circumferential axon guidance (reviewed in (Killeen and Sybingco, 2008)). Furthermore, the L1 orthologs SAX-7 (Sasakura et al., 2005) and LAD-2 (Wang et al., 2008), the *zig* gene products (Aurelio et al., 2002), WRK-1 the Wrapper/Klingon ortholog (Boulin et al., 2006), RIG-3, which is similar to *Drosophila* Klingon and Wrapper (Babu et al.) and finally SYG-1 and SYG-2, the Neph1 and Nephrin homologs (Shen et al., 2004), control key events that contribute to the implementation of nervous system architecture.

The contactin subgroup of IgCAMs consists of glycophosphatidylinositol (GPI) membrane anchored glycoproteins with 4 FNIII-type and 6 Ig modules. Contactins mediate fundamental processes like axon guidance, outgrowth, neuronal migration and formation of axoglial interactions in myelinated fibers (Karagogeos, 2003; Shimoda and Watanabe, 2009). In flies, DContactin is required for septate junction organization and paracellular barrier function in epithelia (Faivre-Sarrailh et al., 2004). Contactins display homophilic and heterophilic interactions and function as glycophosphatidylinositol (GPI)-anchored and released forms (Denaxa et al., 2001; Furley et al., 1990; Karagogeos, 2003). They associate with various transmembrane proteins and relay signals from the extracellular environment. However, the intracellular pathways that mediate signaling via contactins remain elusive.

To gain insight into the function of contactins we focused on RIG-6, the ortholog and the *sole* member of the contactin subgroup in *C. elegans*. Because of its stereotyped and exceptionally well characterized connectome (White et al., 1986), as well as the absence of functional redundancy due to a single gene, the nematode offers an advantageous system for studying the function of contactins. Aiming to elucidate RIG-6 intracellular

* Corresponding author. at: Institute of Molecular Biology and Biotechnology, Foundation for Research and Technology, Hellas, N. Plastira 100, Vassilika Vouton, PO Box 1385, Heraklion 70013, Crete, Greece. Fax: +30 2810 394530.
** Corresponding author. Fax: +30 2810 391067.
E-mail addresses: tavernarakis@imbb.forth.gr (N. Tavernarakis), karagoge@imbb.forth.gr (D. Karagogeos).

0012-1606/$ - see front matter © 2012 Elsevier Inc. All rights reserved.
http://dx.doi.org/10.1016/j.ydbio.2012.10.027

pathway we find that RIG-6 and the cytoskeleton binding protein UNC-53/NAV-2 (Stringham and Schmidt, 2009) may act together in axon guidance in *C. elegans*. UNC-53 (Hekimi and Kershaw, 1993; Stringham et al., 2002; Stringham and Schmidt, 2009) and RIG-6 have overlapping expression patterns and their depletion causes similar phenotypes.

In this study, we show that RIG-6 is important for neuronal as well as non-neuronal cell migration and that RIG-6 optimal expression is critical for its function. Our data directly implicate RIG-6 in mechanosensory axon outgrowth as well as commissure navigation. Moreover, we show that RIG-6 inhibits excretory canal cell tubular elongation. This finding reveals a novel role of contactin in tubulogenesis/cell morphogenesis, which may also be important in other organisms.

Materials and methods

Strains and genetics

We used standard methods for *C. elegans* maintenance, crosses and other genetic manipulations (Brenner, 1974). Nematodes were cultured at 20 °C with the exception of the cold sensitive *rig-6(ok1589)* and *rig-6(gk376)* mutants (and necessary control populations) which were grown at 15 °C. The *Escherichia coli* strain OP50 was used as a food resource. We used hermaphrodite worms for all analyses. The following strains were used: N2: wild-type Bristol isolate, VC1125: *rig-6(ok1589)II*, VC884: *rig-6(gk376)II*, MT152: *unc-53(n152)II*, VH715: *hdIs17*[p_{glr-1}YFP p_{unc-47}YFP $p_{unc-129}$YFP pRF4]*I*; *hdIs10*[$p_{unc-129}$CFP p_{glr-1}YFP p_{unc-47}DsRed p_{hsp-16}pRF4]*V*; *nre-1(hd20)X lin-15b(hd126)X*, *hdIs17I; unc-53(n152)II; hdIs10V*, *SK4005: zdIs5*[p_{mec-4}GFP]*I*.

The following transgenic lines were used in this study: *zdIs5*[p_{mec-4}GFP]*I; rig-6(ok1589)II*, *Ex*[p_{rig-6}RIG-6::GFP pRF4], *Ex*[p_{rig-6}RIG-6 p_{myo-2}GFP], *zdIs5*[p_{mec-4}GFP]*I; Ex*[p_{rig-6}RIG-6 pRF4], *zdIs5*[p_{mec-4}GFP]*I; unc-53(n152)II; Ex*[p_{rig-6}RIG-6 pRF4], *hdIs17I; hdIs10V; Ex*[p_{rig-6}RIG-6 p_{myo-2}GFP], *zdIs5*[p_{mec-4}GFP]*I; Ex*[p_{mec-17} RIG-6b,d pRF4], *Ex*[p_{rig-6}RIG-6 p_{mec-17}DsRed::SNB-1 pRF4], *Ex* [p_{rig-6}RIG-6 p_{pgp-12}GFP pRF4], *rig-6(ok1589)II; Ex*[p_{pgp-12}GFP pRF4], *Is*[p_{unc-47}GFP]*X Is*[p_{unc-47}GFP]*X*; *Ex*[p_{rig-6}RIG-6 pRF4] and *zdIs5*[p_{mec-4}GFP]*I; rig-6(ok1589)II; Ex*[p_{mec-17}RIG-6b,d pRF4]. *hdIs17I; hdIs10V* transgene was obtained by outcrossing VH715 with N2 worms 4 times.

Plasmids and RNAi

For the construction of the p_{rig-6}RIG-6::GFP chimera, we fused GFP at the carboxy terminus of the RIG-6 protein. The translational fusion encompasses the C33F10.5d isoform sequence, excluding the stop codon, and 2.1 kb of upstream sequence. Since all the isoforms share the same last exon, the cloning of the sequence of the largest isoform ensures that the 5 isoforms are simultaneously expressed under their endogenous promoter in fusion with GFP. The sequence was amplified by PCR from N2 genomic DNA, in two fragments. The two partially overlapping fragments were cloned sequentially into *Sac*II–*Not*I and *Not*I–*Sal*I sites of pBluescript KS. The primers that we used incorporated the appropriate restriction enzymes sites for the subcloning. The primers used for the first fragment are: 5′CCCCCGCGGTAAACTG AAACTTTGATTTACA3′ and 5′GAATGCGGCCGCCTTTGGCTAATCAC GATTGA3′ while for the second fragment are 5′GAATGCGGCCG CAGATTTATGTAGGTGCCCATCAT and 5′CCGCGTCGACGAGTCTCCA TAGTAATAATAACA3′. In a third step the plasmid was digested with *Afe*I and self-ligated. Finally the *Sac*II blunted—*Sal*I fragment was subcloned into the *Hin*dIII filled in- *Sal*I sites of the pPDB95.77 vector (Fire et al., 1990). The final plasmid was co-injected with the *rol-6(su1006)* transformation marker (pRF4 plasmid) at 100 ng μl^{-1} each. For expression pattern analysis we examined 7 transgenic lines.

For the overexpression of *rig-6*, we used the *pBluescript KS-rig-6* plasmid mentioned above. The *Sal*I–*Bam*HI fragment was removed and substituted with the PCR amplified fragment that contained the stop codon and the 3′UTR of C33F10.5d. The primers used included *Bam*HI and *Sal*I restriction sites, respectively as follows: 5′TCGGGATCCGAAATCTCTGCAACT3′and 5′ACGCGTCGACCTGCCACAGCCATTGCTCAAG3′.The *rig-6* overexpressing plasmid was co-injected with a p_{myo-2}GFP or pRF4 plasmid at 60 ng μl^{-1} and 50 ng μl^{-1}, respectively. In each case, at least 3 lines were examined and data from one representative line are shown.

For excretory canal visualization, we used a p_{pgp-12}GFP transcriptional fusion. The *pgp-12* promoter was amplified with PCR using the primers 5′CCCAAGCTTTGTGCTTGCAGTGAACCAGA3′ and 5′GCGGATCCACGCCACTTCATGTTTAACC3′ that introduce *Hin*dIII and *Bam*HI restriction sites. The fragment was cloned into the respective restriction sites of the pPD95_77 vector. The resulting plasmid was co-injected with p_{rig-6}RIG-6 and pRF4 plasmids in 50, 60 and 50 ng μl^{-1}, respectively.

The p_{pgp-12}DsRed reporter plasmid was generated by cloning the *pgp-12* promoter to pPD95.77-DsRED (Fire et al., 1990). The resulting plasmid was injected in 50 ng μl^{-1}.

For the p_{pgp-12}RIG-6 rescuing construct we substituted the *mec-17* promoter from the p_{mec-17}RIG-6bd plasmid (please see below) with the *pgp-12* promoter. The resulting construct was injected with p_{pgp-12} GFP in 5 and 50 ng μl^{-1}, respectively.

To express *rig-6* specifically in the touch receptor neurons, we utilized the *mec-17* gene promoter. The1643 bp, PCR-amplified, *mec-17* promoter was initially cloned into the PCRII-Topo vector and was subcloned in to pBluescript 2SK, following a *Sac*I, *Not*I digestion. The primers used for subcloning the *mec-17* promoter were: 5′ GGATCCAGCAAAGACGGCAAGAACTG 3′ and 5′ GGTACC-GATCGAATCGTCTCACAACT 3′ (the *Bam*HI/*Kpn*I sites that were introduced in the amplified fragment were not used in this cloning step). We amplified the *rig-6* genomic sequence and the 3′ UTR using the following primers: 5′GAATGCGGCCGCATGA-TGATGCTTATTCGGTGT3′ and 5′ACGCGTCGACCTGCCACAGCCA-TTGCTCAAG3′ using the previous mentioned overexpressing construct as template. The primers introduced *Not*I and *Sal*I restriction sites to the PCR fragment, which was cloned into the pBluescript 2SK vector downstream of the *mec-17* promoter. In the final step, the plasmid was digested with *Sph*I and self-ligated to remove the *rig-6*a promoter and first exon. The resulting construct was co-injected in *zdIs5*[p_{mec-4}GFP]*I* worms with pRF4 plasmid at 60 ng μl^{-1} and 50 ng μl^{-1}, respectively. For the rescue of *rig-6(ok1589)* axon outgrowth phenotype we injected the p_{mec-17}RIG-6 transgene at 5 ng μl^{-1}. No less than 3 transgenic lines were visualized and data from one line are shown.

To test if *rig-6* is expressed in touch receptor neurons, we co-expressed p_{rig-6}RIG-6::GFP together with p_{mec-17}DsRED::SNB-1. For the generation of the later construct we used the plasmid pPD95.77-DsRED::SNB-1 described previously (Voglis and Tavernarakis, 2008). The *mec-17* promoter was isolated from PCRII-Topo-p_{mec-17} plasmid following *Bam*HI/*Kpn*I digestion and subcloned upstream of dsRed at the respective cloning sites.

For *rig-6* RNAi experiments, a plasmid that drives the synthesis of double stranded RNA was used to transform the *Escherichia coli* strain HT115(DE3) as previously described (Kamath et al., 2001). A 2.7 kb fragment was amplified by PCR from N2 genomic DNA, using the primers 5′CTAGCTAGCCTATGCCTGCTCACTTTCTGTC3′ and 5′CTAGCTAGCCTGAAGTTCGATGGATGACCAT3′. The fragment was cloned into the pL4440 vector (Timmons and Fire, 1998), at the *Nhe*I restriction site. Nematodes were fed with transformed

HT115 *E. coli* bacteria and young adults of the F2 generation were scored. We monitored the effect of *rig-6* RNAi on the touch receptor neurons, Distal Tip Cell migration and the excretory canal in wild type animals. The RNAi sensitive strain VH715 (see stains and genetics) (Schmitz et al., 2007)was used for VNC.

Anatomical analysis

Commissure branching of VNC motorneurons was considered defective if three or more axons formed branches. The abnormal midline crossing of axons from the one VNC trajectory to the other is defined as "cross-over defect". The abnormal trajectory of commissural axons is defined as "commissure navigation".

To measure PLM axon outgrowth we defined three length categories; wild type, for PLM axon termination anterior to the vulva; moderate truncation, for axon termination between the vulva and PVM cell body; and severe truncation for axon termination posterior to the PVM cell body. ALM length was considered as truncated when the anterior processes did not pass over the nerve ring branch. To monitor excretory canal elongation, we defined three length categories; severe truncation, for termination of excretory tubes before the vulva; moderate truncation, for termination before the end of the gonad arm; and wild type for termination between the end of the gonad and the tail of the animal.

Behavioral assays

To assay egg laying, we used synchronized cultures of N2 and *Ex*[$p_{rig\text{-}6}$RIG-6, $p_{myo\text{-}2}$GFP] worms. Animals were transferred in fresh OP50 plates every eight hours starting from the L4 stage and their eggs were counted. To examine locomotion, synchronized age-matched animals were transferred in fresh plates and were left to cut tracks on the bacterial lawn. Videos of moving worms (1 min duration each) were obtained and analyzed using the Nemo software as described previously (Tsibidis and Tavernarakis, 2007). For each strain 10 trials were conducted.

Microscopy analysis

Animals were mounted in 2% agarose pads after anesthetization with 10 mM NaN3. Worms were observed using a Zeiss Axionscop epifluorescence microscope and pictures were obtained using an Axiocam camera or the Bio-Rad Radiance 2100 scanhead, (Bio-Rad, Hercules, USA) and the Bio-Rad Laser-Sharp 2000 software.

Statistical analysis

Experiments were repeated at least 3 times and statistical analyses were performed using the GraphPad Prism software package (GraphPad Software Inc., San Diego, USA) and the Microsoft Office 2003 Excel software package (Microsoft Corporation, Redmond USA). Analysis of variance (ANOVA) was used for comparisons of multiple groups of values, followed by Bonferroni multiple-group comparison tests.

Results

The contactin RIG-6 is expressed in neuronal and non-neuronal cells

rig-6 encodes 5 alternative splice variants, a, b, c, d1 and d2 (Fig. 1A). All variants include 4 fibronectin type III domains at their carboxy-terminus and 3 to 6 immunoglobulin-like domains at the amino-terminus. Variants a and d are predicted to be GPI anchored to the membrane (Fig. 1B and C). All *rig-6* isoforms have the cleavable ω site at their carboxy-terminus but only isoforms a

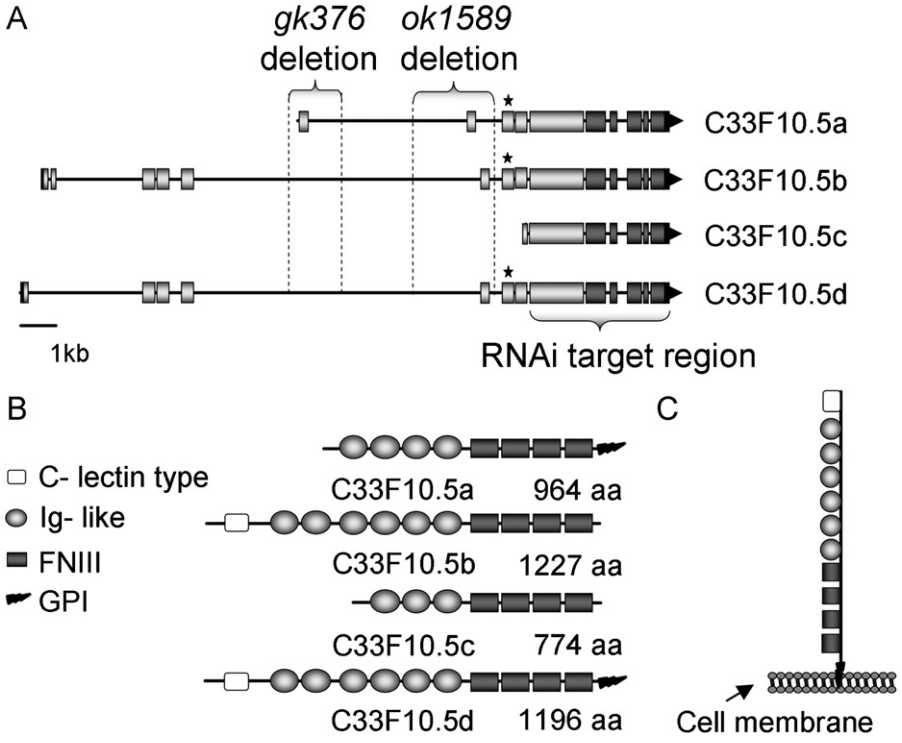

Fig. 1. *rig-6* genomic organization. (A). Schematic representation of *rig-6* alternative splice variants a, b, c and d. Dashed lines indicate the deleted genomic regions in the *gk376* and *ok1589* alleles. The *ok1589* deletion causes the formation of a premature stop codon (asterisk) in isoforms a, b and d. The *rig-6* genomic region targeted by RNAi is also shown. (B). Schematic diagram showing the predicted protein domains of RIG-6 isoforms in the wild type. (C). Topology of the GPI-anchored RIG-6d isoform at the cell membrane.

and d have the amino-terminal signal sequence, which targets the peptide to the ER. We used the hypomorphic *rig-6(ok1589)* mutant allele, which contains a 1554 bp deletion affecting isoforms a, b, and d, by generating premature stop codons and truncated protein products (Fig. 1A). We also examined the weak *rig-6(gk376)* mutant strain. *gk376* deletion knocks down the expression of the *rig-6a* variant, whereas it does not affect the expression of other isoforms (Fig. 1A).

To determine the *rig-6* spatiotemporal expression pattern, we generated a full-length translational GFP reporter fusion (Fig. 2A). The $p_{rig\text{-}6}$RIG-6::GFP construct drives expression of all RIG-6 isoforms in fusion with GFP, under their endogenous promoter (Table S1). *rig-6* expression is detected during embryogenesis (Fig. 2B) and is maintained throughout adulthood. *rig-6* is expressed in I1 and I3 pharyngeal interneurons, NSM motor neurons and other unidentified head neurons (Fig. 2C and data not shown). RIG-6::GFP is also localized in the cell bodies and axons of different subtypes of VNC motorneurons (Fig. 2E), in the HSN and the CAN neurons (Fig. 2F and D). Neuronal expression of *rig-6* also includes the ALM (Fig. 2H–J) and PLM (Fig. 2K–M) touch receptor neurons.

Non-neuronal cells expressing *rig-6* include somatic muscles and the hypodermis (Fig. 2D, arrowhead and G, arrow). We also detected *rig-6* expression in the developing and adult EC: $p_{rig\text{-}6}$RIG-6::GFP fusion is co-expressed with the EC specific $p_{pgp\text{-}12}$dsRed reporter (Fig. 2N–P).

RIG-6 is required for EC tubular elongation

In *C. elegans* excretion and osmotic balance are regulated by a single cell, the "H"-shaped EC, which expresses contactin (Fig. 2N). Canal cell development and morphogenesis involves DV and AP migration of the canal tips, which, when fully developed, reach the head and the tail of the animal (Buechner, 2002) (Fig. 3A). RIG-6 expression in the EC prompted us to examine its role on EC cell migration. Using a $p_{pgp\text{-}12}$GFP reporter transgene we observed that 63% of *rig-6(ok1589)* mutants have defective elongation of posterior excretory canals (Fig. 3B and F). A less penetrant, canal outgrowth defect is observed in the weaker *gk376* mutants (Fig. 3F) suggesting that this phenotype is specific to RIG-6 depletion. *rig-6* RNAi knockdown also caused excretory canal truncation. RNAi targets the carboxy-terminal sequence that is common to all *rig-6* variants (Fig. 1A). Specifically, 21% of *rig-6(RNAi)* animals had truncated canals. 7,5% of the control animals had shorter canals ($p < 0.05$, unpaired t test).Thus, tubular elongation of the single-cell EC requires RIG-6.

To test whether expression of RIG-6 specifically in the EC can rescue the canal truncation phenotype of *rig-6(ok1589)* mutants,

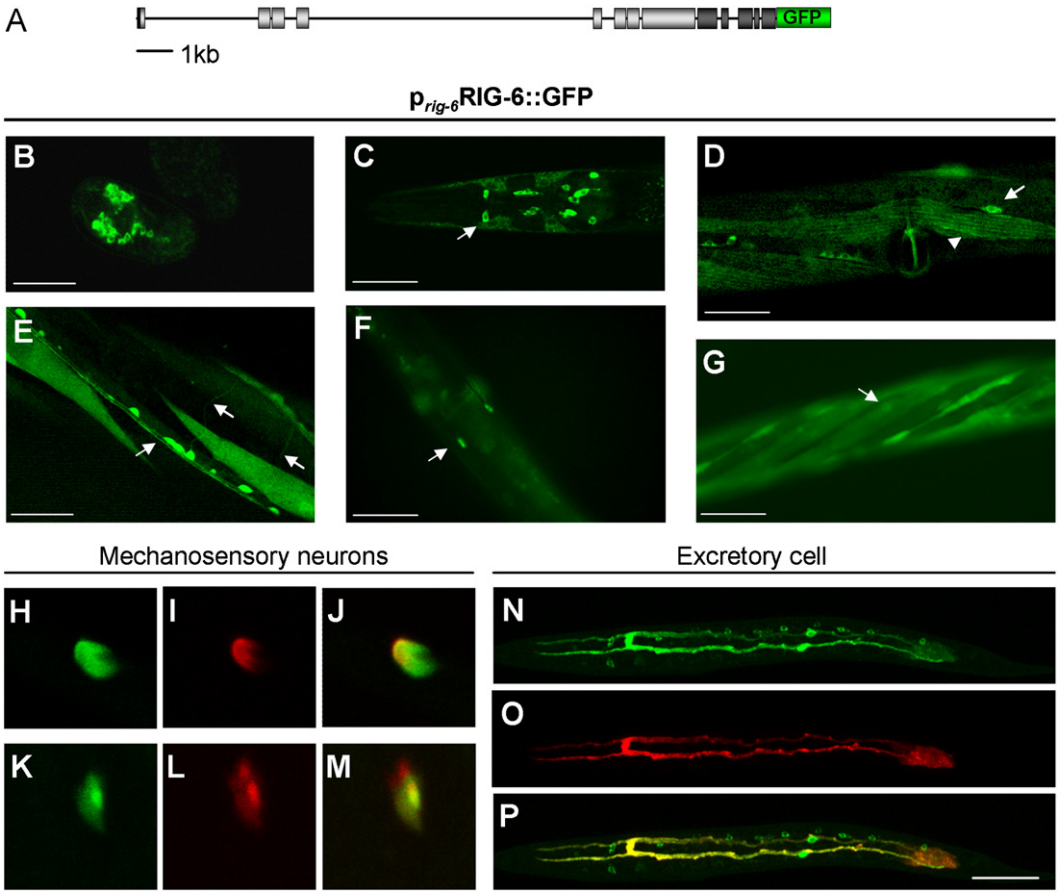

Fig. 2. *rig-6* spatiotemporal expression pattern. (A). Schematic of the full-length *rig-6*::GFP reporter fusion used to determine the spatiotemporal *rig-6* expression pattern. (B). *rig-6* expression begins from embryonic stages and it is maintained throughout adulthood. *rig-6* is expressed in neural precursors. Neuronal expression includes several head neurons including the NSM (C), CAN neurons (D) VNC motorneurons and commissures (E) and HSN neurons (F) (arrows). (H)–(M). *rig-6* expression in the ALM (H)–(J) and PLM (K)–(M) touch-receptor cells is shown by co-injection of $p_{rig\text{-}6}$RIG-6::GFP and $p_{mec\text{-}17}$:DsRed::SNB-1 reporter plasmids in wild type worms. (I), (L). The DsRed::synaptobrevin chimera is expressed under the *mec-17* promoter in ALM and PLM neurons, respectively abd it is detected both in synapses and cell bodies. (J), (M). RIG-6::GFP and DsRed::SNB-1 are co-expressed in ALM and PLM neurons in the 80% of the examined animals. Non-neuronal *rig-6* expression includes the hypodermis (arrow) (G), body wall muscles (D) (arrowhead) and the excretory canal (N)–(P). N. $p_{rig\text{-}6}$RIG-6::GFP expression in the excretory canal of a L1 larva. (O). $p_{pgp\text{-}12}$dsRed expression in the excretory canal. (P). $p_{rig\text{-}6}$RIG-6::GFP is co-expressed with $p_{pgp\text{-}12}$dsRed. Scale bars: (B) 100 μm; (C) 100 μm; (D), (F) 110 μm; (E) 30 μm; (G) 80 μm; (E), (F), (G) 50 μm.

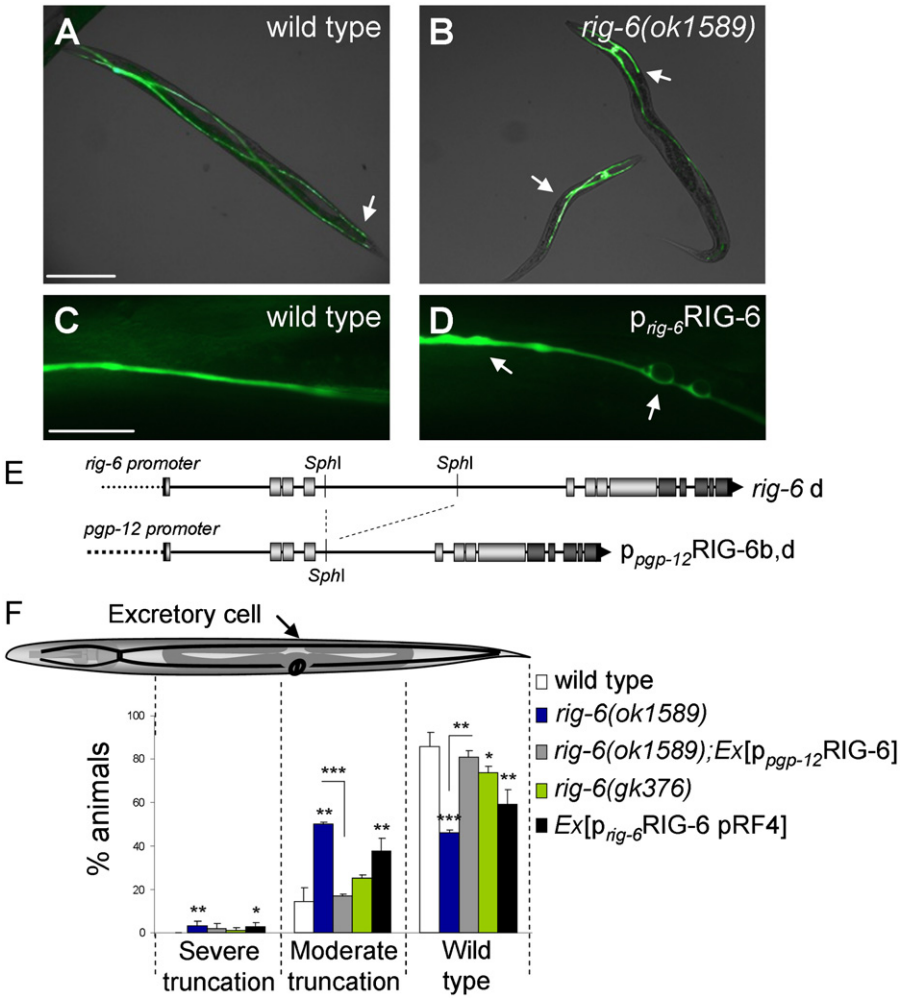

Fig. 3. RIG-6 mediates EC development. (A)–(D). RIG-6 depletion and increase cause impaired outgrowth of the excretory canals. The excretory canal cell is visualized using the p_{pgp-12}GFP transgene. Excretory canal termination points are indicated by arrows. (A). In wild type animals, anterior and posterior canals reach the head and the tail of the animal, respectively. (B). *rig-6(ok1589)* mutants have truncated posterior canals. (C). Wild type canals have a uniform width. (D). *rig-6* overexpression causes the formation of cysts as indicated by arrows. (E). Schematic of the wild type *rig-6* d isoform and the p_{pgp-12}RIG-6b,d transgene. In the later, the *Sph*I fragment was removed to avoid endogenous expression of isoform a (for details see Methods). (F). Schematic diagram showing the EC of a wild type animal. RIG-6 deficiency and excess lead to a premature termination of the posterior canals which were grouped in three categories (wild type, moderate truncation and severe truncation) according to their length, as indicated by dashed lines. *rig-6* expression under the *pgp-12* promoter rescues canal truncation in *rig-6(ok1589)* mutants. Numbers indicate the mean percentile of animals. Error bars denote SEM (* $P<0.05$, ** $P<0.01$, unpaired *t*-test). Scale bars: (A), (B) 220 μm; (C), (D) 50 μm.

we expressed RIG-6 b, d1 and d2 isoforms under the EC-specific *pgp-12* promoter (Fig. 3E). We observed that *rig-6(ok1589)*; *Ex*[p_{pgp-12}RIG-6] transgenic animals show normal development of the excretory canal. This data show that *rig-6* expression in EC is required for accurate tubular elongation (Fig. 3F).

Imbalance in adhesion molecule stoichiometry often perturbs cell migration and guidance. Aiming to test whether RIG-6 upregulation affects excretory canal development, we generated animals carrying multiple copies of the entire *rig-6* genomic locus (Table S1), incorporating all splice variants and their promoters. We confirmed *rig-6* overexpression by RTq-PCR and found that *rig-6* mRNA levels are 18 fold increased in p_{rig-6}RIG-6 animals in comparison with wild type animals (not shown).

We observed that excretory canals terminate prematurely in 40% of *rig-6* overexpressing animals (Fig. 3F). While wild type canals have a uniform width along their structure, *rig-6*-overexpressing worms show excretory canals of variable width and occasional formation of cysts along the canal arms (Fig. 3D). Thus, both RIG-6 depletion and overexpression perturb tubular elongation and EC cell morphogenesis.

An additional phenotype of non-neuronal cell migration which shares guidance mechanisms with neuronal axons, occurs during gonad development. Gonadal arm elongation is guided by two distal tip cells which migrate both in the AP and DV directions in order to create a U shaped gonad. Given that RIG-6 affects canal outgrowth and migration, we tested whether it also functions in gonad formation. *rig-6(ok1589)* and *rig-6(RNAi)* animals have low penetrance distal tip migration defects (Fig. S1). Taken together, our findings reveal for the first time that a contactin member (RIG-6) is important for non-neuronal cell migration.

RIG-6 affects axon growth and guidance along the longitudinal and circumferential axon

We examined whether *rig-6* is required for proper nervous system development in nematodes. To test if RIG-6 is involved in axon outgrowth along the anterior–posterior (AP) axis, we followed the development of the six mechanosensory neurons of *C. elegans* which express *rig-6* (Fig. 2H–M). We used p_{mec-4}GFP transgenic animals which express GFP under the mechanosensory

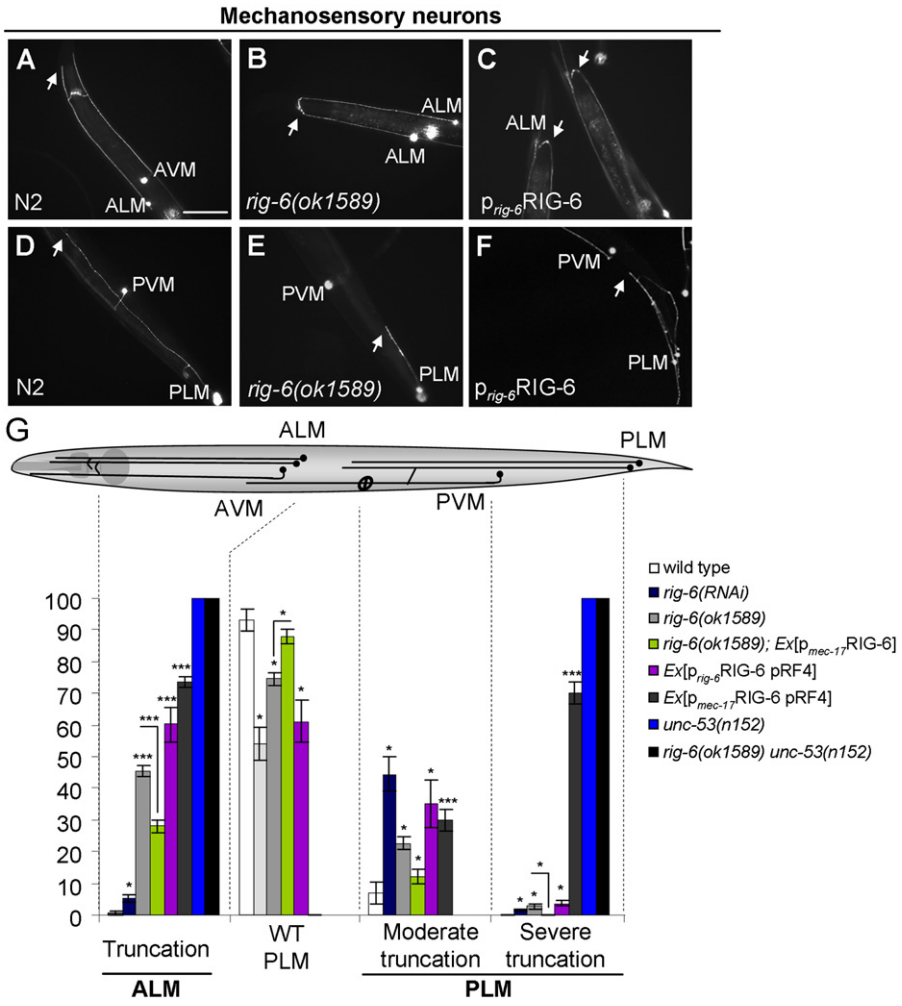

Fig. 4. RIG-6 imbalance causes mechanosensory neuron truncation. (A)–(F). *rig-6* depleted and overexpressing animals have truncated ALM and PLM axons, visualized using a p_{mec-4}GFP reporter. (A), (D). Images showing wild type ALM, AVM and PLM, PVM neurons, respectively (arrows indicate axon termination points). (B), (E). *rig-6(ok1589)* mutants have shortened (B) ALM and (E) PLM projections (arrow). PVM axon is out of focus in (E). (C), (F). *rig-6* overexpressing animals have also truncated ALM and PLM axons. Scale bars A-F 110 μm. (G). Schematic of the 6 touch-receptor neurons in the wild type animal. ALM axons were defined as "truncated" if they terminated before or in the area of the nerve ring. Truncated PLM axons were separated in three categories (wild type, moderate truncation, severe truncation) according to their length, as defined by the dashed lines. *rig-6* overexpression under the mechanosensory neuron specific *mec-17* promoter rescues axon truncation in *rig-6(ok1589)* mutants. p_{mec-17}RIG-6 refers to different arrays in *Ex*[p_{mec-17}RIG-6] and *rig-6(ok1589);Ex*[p_{mec-17}RIG-6] animals (injected at high and low concentration, respectively). Numbers indicate the mean percentile of animals showing abnormalities (error bars denote SEM). Asterisks indicate statistically significant differences between *rig-6* mutants and wild type animals for a certain axon length category (* $P<0.05$, ** $P<0.01$, *** $P<0.005$, unpaired *t*-test).

neuron specific *mec-4* gene promoter (Fig. 4A–F). In wild type animals, ALML/R cell bodies are positioned in the middle of the body and extend a single axon in a dorsal sublateral tract to a final destination above the nerve ring (Fig. 4A). In the nerve ring, they extend a branch that forms synapses with other neurons. PLML/R cell bodies are positioned in the tail ganglion and extend a dendrite in a ventral sublateral tract that is terminated between the ALM body and the vulva (Chalfie et al., 1985) (Fig. 4D). We found that 45% of *rig-6(ok1589)* mutant worms have truncated ALM axons that do not extend above the nerve ring (Fig. 4B and G). Truncated PLM anterior processes were observed in 23% of the animals. We also confirmed the above phenotypes by RNAi against *rig-6* in p_{mec-4}GFP worms (Fig. 4G). PVM axons defects were not visualized in the mutant, while occasionally the tips of AVM axons were folded back at the head of the animal. Combined, our observations suggest that *rig-6* is required for ALM and PLM axon outgrowth.

Next we investigated whether RIG-6 expression is required in the mechanosensory neurons for their proper axon outgrowth. We tested whether targeted expression of *rig-6* in the touch receptor neurons can rescue the axon outgrowth phenotype. Expression of RIG-6 b, d1 and d2 isoforms specifically in touch receptor neurons under the *mec-17* gene promoter is sufficient to significantly rescue axon elongation of ALM and PLM neurons in *rig-6(ok1589)* mutants (Fig. 4G). Our results suggest that *rig-6* expression is required in the touch receptor neurons for accurate axon development.

Interestingly, we observed that overexpressing of *rig-6* under the *mec-17* promoter, exhibits pronounced axon outgrowth defects in wild type animals. 73% of these animals had truncated ALM axons. Moreover, 70% of PLM axons ended abruptly soon after the beginning of their trajectory (Fig. 4G). PLM processes of normal length were absent. Upregulation of *rig-6* expression under its endogenous promoter in wild type background also inhibits mechanosensory axon elongation. Animals carrying multiple copies of the entire *rig-6* genomic locus exhibited significant axon outgrowth defects in the mechanosensory neurons. 60% of *rig-6*-overexpressing animals had truncated ALM axons (Fig. 4C and G) and 40% had shorter PLM axons (Fig. 4F and G). Thus mechanosensory axon outgrowth is affected by *rig-6* concentration levels.

To determine whether RIG-6 is involved in dorso-ventral (DV) axon outgrowth and navigation, we examined *rig-6* expressing motorneurons and the VNC of animals carrying a transgene (*hdIs17I;hdIs10V*, see Methods) which drives the expression of fluorescent proteins under the *unc-47*, *unc-129* and *glr-1* gene promoters in D-type motorneurons, DA/DB motorneurons and *glr-1* interneurons, respectively (Schmitz et al., 2007). In wild type animals, the VNC consists of two separate tracts (left and right). The majority of axons pass through the right tract, with only a few axons comprising the left tract. Motorneuron cell bodies are positioned in the middle, defining the midline and their commissures follow a circumferential trajectory (Fig. 5A) (White et al., 1976). We detected abnormal navigation of commissural axons in 16% of mutant worms, consistent with a previous study (Schwarz et al., 2009) (Fig. 5B). Furthermore, we observed that 5% of *rig-6(ok1589)* mutants have right tract axons that cross abnormally the midline and join the left bundle (Fig. 5C, the same phenotype is shown for *rig-6(RNAi)* animals). RNAi knockdown of RIG-6 in a RNAi sensitive strain (Schmitz et al., 2007) reproduced these phenotypes (see Fig. 7E as well). Our data indicate a specific involvement of RIG-6 in the DV patterning of the nervous system.

We also examined the impact of *rig-6* overexpression on VNC structure. Commissures of motorneurons were misguided and branched in 25% and 27% of the animals, respectively (Fig. 5E and Fig. 7E). In addition, 24% of *rig-6*-overexpressing animals show cross-over defects in the VNC (Fig. 5F and Fig. 7E), a phenotype also observed in *rig-6* mutant animals.

The implication of RIG-6 in longitudinal migration prompted us to follow the development of individual subsets of motorneurons such as DD motorneurons. Projections of these neurons extend both in anterior and posterior direction upon reaching the DNC (Fig. 5G) (Von Stetina et al., 2006). We visualized DD motorneurons using a p_{unc-47}GFP transgene in L1 larvae. Excess RIG-6 inhibited exclusively the posterior extension of DD motorneuron processes in about 50% of the examined animals (Fig. 5H). In addition, *rig-6* overexpression caused DD commissural axon misrouting and branching (Fig. 5H). Thus, *rig-6* upregulation causes severe axon guidance, outgrowth and branching defects in the VNC. Our data show that both RIG-6 depletion and overexpression result in impaired axon elongation and navigation, suggesting that optimal regulation of RIG-6 levels is critical for proper nervous system development.

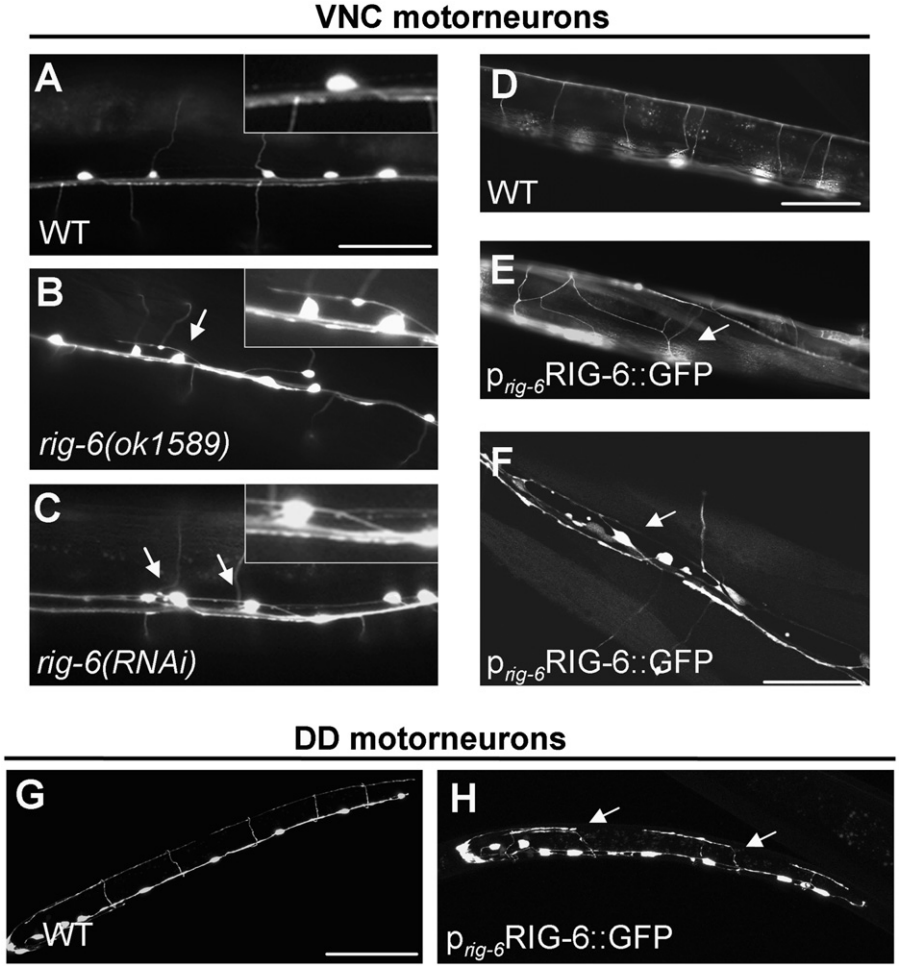

Fig. 5. RIG-6 depletion and up regulation cause impaired axon guidance and outgrowth of VNC motorneurons .(A)–(F). VNC architecture was visualized using the *hdIs17I* and *hdIs10V* transgenes (Schmitz et al., 2007). (A). GFP expressing axons run fasciculated in the right trajectory of the VNC. Commissural axons follow a circumferential trajectory. (B). Motorneuron commissures in *rig-6(ok1589)* mutants are misguided (arrows). Their dorsal parts are out of focus. (C). In both *rig-6(ok1589)* and *rig-6(RNAi)* animals, axons from the right bundle cross over to the left as indicated by arrows (shown for *rig-6(RNAi)* animals). Inserts show higher magnification of panels (A), (B), and (C), respectively. (D). Image of wild type dorsal nerve cord and commissural axons visualized using the *hdIs17I* and *hdIs10V* transgenes. (E). *rig-6* overexpression results in misguided commissural axons, which join and form branches (arrows). (F). Axon cross-over is observed in the VNC of *rig-6*-overexpressing animals (arrow). (G), (H). DD motorneurons were visualized using p_{unc-47}GFP transgene. (G). Wild type L1 larvae showing DD motorneuron cell bodies and processes. (H). In *rig-6* overexpressing animals DD motorneuron processes do not elongate in the posterior direction as indicated by arrows. Their processes converge and form branches. Scale bars: (A)–(C) 50 μm; (D), (E) 110 μm; (F)–(H) 50 μm.

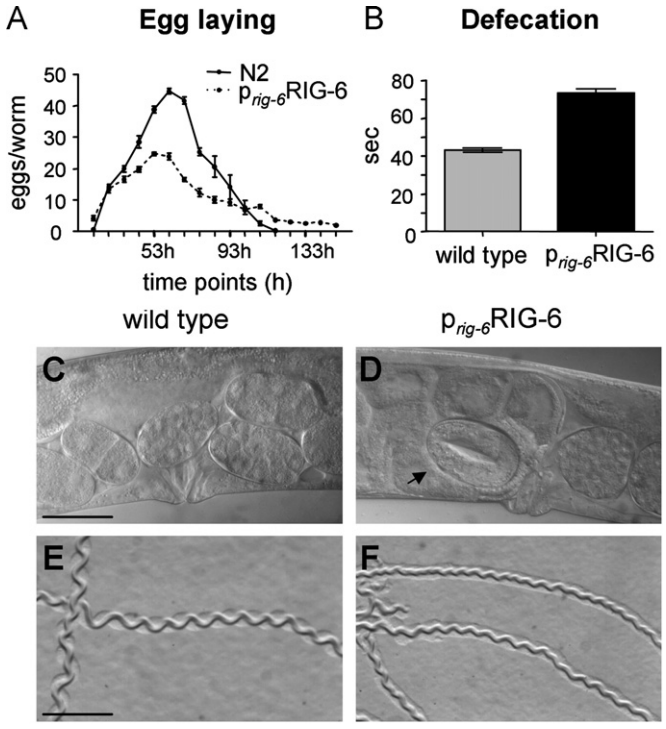

Fig. 6. Increased levels of RIG-6 cause specific behavioral defects. (A). Abnormal egg laying and reduced fertility of *rig-6*-overexpressing worms compared to wild type. The mean number of eggs per worm is plotted for each time point. Error bars denote SEM. The mean total number of the progeny for N2 worms is 260 ± 15, whereas for $p_{rig\text{-}6}$RIG-6 animals, 180 ± 1.22 ($P < 0.05$, unpaired *t*-test). (B). Defecation rhythm is retarded in $p_{rig\text{-}6}$RIG-6 nematodes compared to N2 worms. The mean time interval between successive sphincter muscle contractions is shown in wild type animals and *rig-6*-overexpressing worms. Error bars denote SEM ($P < 0.001$, unpaired *t*-test). (C). Image showing eggs of gravid adult N2 worms just before their exit from the vulva. (D). Three-fold stage embryo (arrow) entrapped in the uterus of a *rig-6*-overexpressing worm. (E). Tracts of wild type worms in fresh bacterial lawns. (F). Tracts of *rig-6* overexpressing worms present decreased amplitude and wavelength. Scale bars: (C), (D) 50 μm; (E), (F) 1 mm.

RIG-6 upregulation affects animal behavior

rig-6-overexpressing worms are generally smaller compared to the wild type animals. These worms often die carrying eggs. Egg laying analysis showed that *rig-6* overexpressing animals are less fertile and lay eggs for longer periods. 50% of the population died carrying embryos, likely due to egg hatching inside the mother (Fig. 6A, C, D). Fluorodeoxyuridine (FUdR), which inhibits DNA synthesis, causing sterility and preventing egg hatching (Hosono, 1978) prevented premature death (not shown).

rig-6 overexpression alters the defecation rhythm by significantly increasing the time interval between successive sphincter contractions (Fig. 6B). In addition, *rig-6*-overexpressing worms show abnormal locomotion, evident by the shorter wavelength and amplitude of tracts inscribed on bacterial lawns (Fig. 6E, F and Table 1). This behavior is consistent with impaired motorneuron development and function in *rig-6*-overexpessing animals. We did not detect locomotion abnormalities (Table 1) or defecation defects in the hypomorphic *rig-6 (ok1589)* mutants.

RIG-6 and UNC-53 in longitudinal and circumferential axon guidance

Aiming to identify intracellular molecules that potentially function together with *rig-6* to mediate axon guidance, we searched for genes with overlapping expression that, when mutated, display similar phenotypes with *rig-6* mutants. *unc-53* encodes a large cytoskeleton binding protein known to affect AP and DV axon guidance and outgrowth (Hekimi and Kershaw, 1993; Stringham et al., 2002). *unc-53* mutants have shortened ALM and PLM processes, truncated excretory canals as well as commissure and cross defects in the VNC (Hekimi and Kershaw, 1993; Stringham et al., 2002). Overall, *unc-53* mutant phenotypes extensively resemble those observed in *rig-6*-deficient or overexpressing animals. Expression patterns of *rig-6* and *unc-53* overlap. Both genes are expressed in touch receptor neurons, VNC motorneurons and the EC (Schmidt et al., 2009; Schwarz et al., 2009; Stringham et al., 2002). UNC-53 has been shown to act cell-autonomously in axon outgrowth and cell migration (Schmidt et al., 2009; Stringham et al., 2002). The involvement of the two genes in both AP and DV axon outgrowth, the cell autonomous function and their overlapping expression patterns, prompted us to investigate whether they synergize to facilitate proper cell migration.

Although, touch neuron cell bodies are located normally in animals carrying the hypomorphic *unc-53(n152)* allele, their axons are always truncated, frequently forming ectopic branches (Hekimi and Kershaw, 1993; Trent et al., 1983). We observed that *rig-6*-overexpressing *unc-53(n152)* mutant worms did not display further shortening of ALM or PLM processes. Nevertheless, we observed that ALM axons form complex tertiary structures in 8.7% of the population (Fig. 7C). Moreover, in 20% of these animals, the AVM axon was twined around the ALM dendrite (Fig. 7D), indicating a severe axon guidance defect. Both phenotypes were absent in single mutants ($P < 0.05$, compared to single mutants, unpaired *t*-test). In addition, we found that *rig-6(ok1589) unc-53(n152)* double mutants did not display significantly different axon outgrowth and navigation defects compared to *unc-53* single mutants (Fig. 4G).

unc-53 mutants overexpressing *rig-6* showed enhanced abnormalities in the VNC. The frequency of cross, commissure branching and commissure navigation defects was significantly (2–3 fold) increased in *rig-6*-overexpressing, *unc-53(n152)* animals compared to single mutants (Fig. 7E). Overall, UNC-53 depletion dramatically enhances the effect of *rig-6* overexpression in both longitudinal and circumferential axon navigation. Together, our findings indicate a phenotypic interaction between RIG-6 and UNC-53 in neuronal patterning during *C. elegans* development.

Discussion

In this study, we examined the involvement of RIG-6 in non-neuronal and neuronal development in *C. elegans*. We report a novel requirement for contactin in cell migration and tubular elongation. We also show that RIG-6 serves an important function in axon outgrowth and navigation along both the AP and DV axis, facilitating accurate mechanosensory neuron and VNC development.

Contactins and nervous system development

Vertebrate contactins are indispensable for proper nervous system formation and function and have been implicated in the pathogenesis of severe neurological disorders. F3/contactin is associated with a lethal congenital myopathy (Compton et al., 2008), TAG-1 is an autoantigen in Multiple Sclerosis (Derfuss et al., 2009) and BIG-2 is correlated with the 3p syndrome and autism (Fernandez et al., 2008; Katidou et al., 2008; Shimoda and Watanabe, 2009). BIG-2 has been also involved in olfactory neuron convergence to the olfactory glomeruli and in olfactory map formation (Kaneko-Goto et al., 2008).

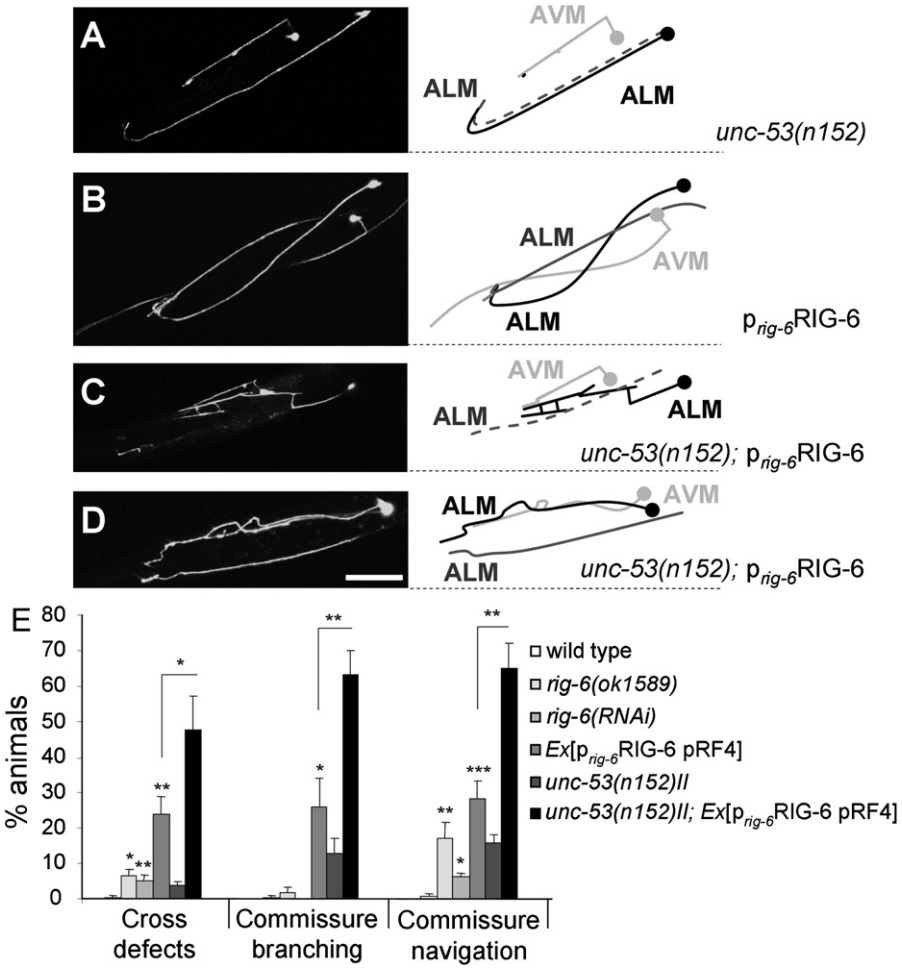

Fig. 7. UNC-53 deficiency exacerbates *rig-6* overexpression phenotypes. (A)–(D).UNC-53 depletion combined with RIG-6 overexpression causes impaired ALM axon branching and guidance. Images of ALM and AVM neurons in *unc-53(n152)* and p_{rig-6}RIG-6 nematodes, as well as their schematic representation are shown. Dashed lines indicate neurons out of the focal plane. (A). *unc-53(n152)* worms have truncated ALM and AVM axons. (B). p_{rig-6}RIG-6 worms also show truncated ALM axons. (C).*rig-6* overexpression in *unc-53(n152)* mutant background causes the formation of tertiary ectopic branches in ALM axons. (D). ALM axon twined around an AVM axon is shown. (E). *rig-6(ok1589)*, *rig-6(RNAi)* and p_{rig-6}RIG-6 animals have cross-over defects and display abnormal commissural navigation at significantly higher frequency, compared to wild type animals. In addition, commissures of p_{rig-6}RIG-6 worms tend to form branches. RIG-6 overexpression considerably enhances the VNC defects of *unc-53(n152)* mutants (for phenotype definition see Materials and Methods). Numbers indicate the mean percentile of animals displaying each phenotype (error bars denote SEM). Asterisks indicate statistically significant differences ($^{*}P<0.05$, $^{**}P<0.01$, $^{***}P<0.005$, unpaired *t*-test). (Scale bar: 50 μm).

Table 1
RIG-6 and animal locomotion.

Genotype	Sinusoidal locomotion wavelength*	Sinusoidal locomotion amplitude*
N2	0.71 ± 0.06	0.38 ± 0.01
rig-6(ok1589)	0.73 ± 0.08	0.36 ± 0.09
N2; *Ex*[p_{rig-6}RIG-6, p_{myo-2}GFP]	0.50 ± 0.04	0.29 ± 0.03

rig-6 overexpression impairs sinusoidal locomotion. p_{rig-6}RIG-6 worms show decreased amplitude and wavelength compared to the tracts of wild type worms ($P<0.001$, unpaired *t*-test). RIG-6 depletion does not affect locomotion.

In *C. elegans*, analysis of multiple IgCAM mutants, using the weak *rig-6(gk376)* allele that affects only the RIG-6a isoform, suggested a functional redundancy among RIG-6 and other IgCAMs in axon navigation at the VNC (Schwarz et al., 2009). Animals carrying the stronger *rig-6(ok1589)* allele alone were also analyzed and displayed variable commissure navigation defects in agreement with our observations (Schwarz et al., 2009). The functional redundancy observed in the VNC may explain the low penetrance commissural misguidance and axon cross-over phenotypes caused by RIG-6 depletion. In our study, we found in addition, that RIG-6 strongly affects mechanosensory axon guidance and DD motorneuron axon elongation as well as EC tubular elongation, which takes place along the longitudinal axis. Thus, RIG-6 appears to influence anteroposterior migration as well as dorsoventral migration.

RIG-6 levels are important in exerting its function

Our data suggest that RIG-6 acts cell autonomously in both EC tubular elongation and axon growth. Cell specific expression of *rig-6* in the excretory canal rescues the canal truncation phenotype while targeted expression of *rig-6* in the touch receptor neurons can rescue the axon outgrowth phenotype observed in *rig-6* mutants. However, cell autonomous studies are highly perplexed in the GPI-anchored/released contactins which have been shown to mediate homophilic and heterophilic complexes in cis and/or in trans (Brummendorf and Rathjen, 1996; Karagogeos, 2003; Kolodkin and Tessier-Lavigne; Shimoda and Watanabe, 2009). Therefore we cannot exclude a parallel non cell-autonomous function of *rig-6*.

We observed that increased levels of RIG-6 have a dramatic impact on nematode neuroanatomy. Both RIG-6 deficiency and excess, impair outgrowth of excretory canals, ALM/PLM axons and proper commissural routing in the VNC, causing a high frequency

of cross over defects. Furthermore, animals expressing RIG-6 under the strong *mec-17* promoter exhibit enhanced axon outgrowth defects in touch receptor neurons, compared to animals expressing RIG-6 under its own weaker promoter. Taken together, our data support that RIG-6 optimal levels are critical for its proper function in vivo. This is possibly due to the modification of homophilic or heterophilic protein complexes that are involved in contact guidance and outgrowth. In particular, homophilic interactions in mammalian contactins have been shown to function in a dominant negative fashion (Denaxa et al., 2001; Kyriakopoulou et al., 2002). It is thus possible that excess RIG-6 functions in a dominant negative fashion, mediating homophilic interactions. Therefore regulation of RIG-6 expression levels is critical for accurate nervous system patterning.

Interestingly and consistent with the above interpretation, both overexpression and depletion of contactin in *Xenopus* cause abnormal development of a subset of primary sensory neurons (Fujita et al., 2000). A dominant negative function has been reported for a truncated form of SAX-7/LAD-1, the ortholog of the IgCAM L1(Chen et al., 2001). SAX-7 is a transmembrane protein. When the three first secreted immunoglobulin domains of SAX-7 are overexpressed, they block endogenous SAX-7 function (Chen et al., 2001).

A dosage dependent effect of extracellular adhesion molecules has been also described for KAL-1 (Rugarli et al., 2002), type XVIII collagen (Ackley et al., 2001), semaphorin MAB-20 (Roy et al., 2000) and Scabrous (Powell et al., 2001). This highlights the importance of precise regulation of the level of expression of extracellular contact cues in axon guidance and migration.

RIG-6 affects C. elegans development and behavior

Behavioral defects are associated with altered RIG-6 levels such as decreased fertility and defecation rhythm as well as abnormal locomotion. The behavioral abnormalities monitored show that defects induced by RIG-6 imbalance are relevant in vivo. Reduced fertility may be caused by impaired spermatheca function (where RIG-6 is expressed) or abnormal gonadal development.

Ventral cord motorneurons control locomotion (Von Stetina et al., 2006). Thus, impaired axonal pattern of motorrneurons and specifically DD motorneurons likely underlies the locomotion defects observed upon RIG-6 upregulation. DD motorneurons regulate sinusoidal locomotion amplitude (McIntire et al., 1993). DD motorneuron axon outgrowth was not inhibited by RIG-6 depletion. It is thus expected to observe normal locomotion in *rig-6* hypomorphic mutants.

We favor the hypothesis that *rig-6* function in the VNC is required developmentally for two reasons. First, cross-over defects induced by RIG-6 imbalance were observed in freshly hatched L1 larvae (not shown), which do not yet develop the axon maintenance phenotype (Aurelio et al., 2002). Second, *rig-6* is expressed in neurons from embryonic stages on. These observations are consistent with the view that RIG-6 is required for axon guidance and not maintenance of VNC architecture.

A novel role for contactins in EC tubular elongation/morphogenesis

RIG-6 imbalance affects non-neuronal cells, such as the EC cell and the gonad distal tip cells. In the case of the former, RIG-6 imbalance causes defective extension of the excretory tubes. Tubulogenesis and axon guidance use common molecular pathways such as Ephrin, Semaphorin and Netrin signaling (Weinstein, 2005). The involvement of RIG-6 in excretory tube extension suggests a novel role for contactins in tubular structure formation, a process important for angiogenesis in higher organisms.

RIG-6 intracellular signaling: A working hypothesis

Several lines of reasoning support the possibility of RIG-6 and UNC-53 synergistic function. First, animals overexpressing *rig-6* share specific phenotypes, such as touch receptor dendrite truncation, incomplete excretory canal elongation, commissure and cross-over defects of VNC motorneurons, egg laying and locomotion abnormalities with UNC-53 deficient mutants. Second both proteins have cell autonomous functions and overlapping expression patterns (Brenner, 1974; Hekimi and Kershaw, 1993; Stringham et al., 2002; Trent et al., 1983). Overall, these intriguing similarities suggest that UNC-53/NAV-2 proteins may contribute to relay signaling via contactins. UNC-53 is homologous to NAV-1, NAV-2 and NAV-3, which mediate axon navigation (Stringham and Schmidt, 2009). Interestingly, contactins and NAVs share overlapping expression in the mammalian nervous system as well (Martinez-Lopez et al., 2005; Yoshihara et al., 1995).

RIG-6 lacks a cytoplasmic tail and it cannot bind physically to the cytoplasmic protein UNC-53. The function of GPI-anchored cell adhesion molecules is known to be controlled by endocytosis (Mayor and Riezman, 2004) and membrane trafficking has been proposed to regulate the function of IgCAMs such as UNC-40, UNC-5 and SAX-3 (Levy-Strumpf and Culotti, 2007; Watari-Goshima et al., 2007). Interestingly, *unc-53* mutants show defective endocytosis in coelomocytes and defective receptor endocytosis by oocytes (Balklava et al., 2007; Fares and Greenwald, 2001). The axon outgrowth and guidance defects in *unc-53* mutants may indicate a role for UNC-53 in endocytosis and trafficking of cell adhesion molecules such as RIG-6. It is has been proposed that a physical interaction of UNC-53 with abi-1 and the actin cytoskeleton could mediate this process (Stringham and Schmidt, 2009). Interestingly, *abi-1* mutants have truncated PLM axons and excretory canals, as well as cross and commissure defects in the VNC, resembling *rig-6* and *unc-53* mutants (Schmidt et al., 2009). Thus, UNC-53 may negatively regulate the abundance of RIG-6 at the cell surface via endocytosis. Consistent with this notion, UNC-53 deficiency further enhances *rig-6* overexpression phenotypes.

Alternatively, RIG-6 may function upstream of UNC-53. However, RIG-6 deficiency does not suppress *unc-53* mutant phenotypes as it would be expected for depletion of genes acting upstream of *unc-53*. This could suggest that other molecules might in parallel regulate axon elongation, ectopic branching and navigation.

Taken together, our data reveal the implication of RIG-6 in fundamental developmental processes, such as tubulogenesis, axon elongation, branching and navigation. The tight evolutionary conservation of this protein family across phyla suggests that contactins may also play an essential role in similar processes in other organisms.

Acknowledgements

We thank A. Pasparaki and E. Vergadi for assistance with experiments. Some nematode strains used in this work were provided by the *C. elegans* Gene Knockout Project at OMRF, which is part of the International *C. elegans* Gene Knockout Consortium, the *Caenorhabditis* Genetics Center, which is funded by the NIH National Center for Research Resources (NCRR), and S. Mitani (National Bioresource Project) in Japan. We thank A. Fire for plasmid vectors. p_{unc-47}GFP animals were kindly provided by J. Culotti. This work was funded by grants from EMBO, the European

Research Council (ERC) and the European Commission to N.T., and by the Marie Curie Training and Mobility Programme (CELL-IMAGE) to D.K. and N.T. and IMBB internal funding to D.K. M.K. is a recipient of the Manasaki Foundation fellowship of the University of Crete.

Author contributions: M.K., N.T. and D.K. designed experiments, analyzed data and wrote the manuscript. M.K. performed experiments.

Appendix A. Supporting information

Supplementary data associated with this article can be found in the online version at http://dx.doi.org/10.1016/j.ydbio.2012.10.027.

References

Ackley, B.D., Crew, J.R., Elamaa, H., Pihlajaniemi, T., Kuo, C.J., Kramer, J.M., 2001. The NC1/endostatin domain of *Caenorhabditis elegans* type XVIII collagen affects cell migration and axon guidance. J. Cell Biol. 152, 1219–1232.

Aurelio, O., Hall, D.H., Hobert, O., 2002. Immunoglobulin-domain proteins required for maintenance of ventral nerve cord organization. Science 295, 686–690.

Babu, K., Hu, Z., Chien, S.C., Garriga, G., Kaplan, J.M., The Immunoglobulin Super Family Protein RIG-3 Prevents Synaptic Potentiation and Regulates Wnt Signaling. Neuron 71, 103–116.

Balklava, Z., Pant, S., Fares, H., Grant, B.D., 2007. Genome-wide analysis identifies a general requirement for polarity proteins in endocytic traffic. Nat. Cell Biol. 9, 1066–1073.

Boulin, T., Pocock, R., Hobert, O., 2006. A novel Eph receptor-interacting IgSF protein provides *C. elegans* motoneurons with midline guidepost function. Curr. Biol. 16, 1871–1883.

Brenner, S., 1974. The genetics of *Caenorhabditis elegans*. Genetics 77, 71–94.

Brummendorf, T., Rathjen, F.G., 1996. Structure/function relationships of axon-associated adhesion receptors of the immunoglobulin superfamily. Curr. Opin. Neurobiol. 6, 584–593.

Buechner, M., 2002. Tubes and the single *C. elegans* excretory cell. Trends Cell Biol. 12, 479–484.

Chalfie, M., Sulston, J.E., White, J.G., Southgate, E., Thomson, J.N., Brenner, S., 1985. The neural circuit for touch sensitivity in *Caenorhabditis elegans*. J. Neurosci. 5, 956–964.

Chen, L., Ong, B., Bennett, V., 2001. LAD-1, the *Caenorhabditis elegans* L1CAM homologue, participates in embryonic and gonadal morphogenesis and is a substrate for fibroblast growth factor receptor pathway-dependent phosphotyrosine-based signaling. J. Cell Biol. 154, 841–855.

Compton, A.G., Albrecht, D.E., Seto, J.T., Cooper, S.T., Ilkovski, B., Jones, K.J., Challis, D., Mowat, D., Ranscht, B., Bahlo, M., Froehner, S.C., North, K.N., 2008. Mutations in contactin-1, a neural adhesion and neuromuscular junction protein, cause a familial form of lethal congenital myopathy. Am. J. Hum. Genet. 83, 714–724.

Denaxa, M., Chan, C.H., Schachner, M., Parnavelas, J.G., Karagogeos, D., 2001. The adhesion molecule TAG-1 mediates the migration of cortical interneurons from the ganglionic eminence along the corticofugal fiber system. Development 128, 4635–4644.

Derfuss, T., Parikh, K., Velhin, S., Braun, M., Mathey, E., Krumbholz, M., Kumpfel, T., Moldenhauer, A., Rader, C., Sonderegger, P., Pollmann, W., Tiefenthaller, C., Bauer, J., Lassmann, H., Wekerle, H., Karagogeos, D., Hohlfeld, R., Linington, C., Meinl, E., 2009. Contactin-2/TAG-1-directed autoimmunity is identified in multiple sclerosis patients and mediates gray matter pathology in animals. Proc. Nat. Acad. Sci. U.S.A. 106, 8302–8307.

Faivre-Sarrailh, C., Banerjee, S., Li, J., Hortsch, M., Laval, M., Bhat, M.A., 2004. Drosophila contactin, a homolog of vertebrate contactin, is required for septate junction organization and paracellular barrier function. Development 131, 4931–4942.

Fares, H., Greenwald, I., 2001. Genetic analysis of endocytosis in *Caenorhabditis elegans*: coelomocyte uptake defective mutants. Genetics 159, 133–145.

Fernandez, T., Morgan, T., Davis, N., Klin, A., Morris, A., Farhi, A., Lifton, R.P., State, M.W., 2008. Disruption of Contactin 4 (CNTN4) results in developmental delay and other features of 3p deletion syndrome. Am. J. Hum. Genet. 82, 1385.

Fire, A., Harrison, S.W., Dixon, D., 1990. A modular set of lacZ fusion vectors for studying gene expression in *Caenorhabditis elegans*. Gene 93, 189–198.

Fujita, N., Saito, R., Watanabe, K., Nagata, S., 2000. An essential role of the neuronal cell adhesion molecule contactin in development of the Xenopus primary sensory system. Dev. Biol. 221, 308–320.

Furley, A.J., Morton, S.B., Manalo, D., Karagogeos, D., Dodd, J., Jessell, T.M., 1990. The axonal glycoprotein TAG-1 is an immunoglobulin superfamily member with neurite outgrowth-promoting activity. Cell 61, 157–170.

Hekimi, S., Kershaw, D., 1993. Axonal guidance defects in a *Caenorhabditis elegans* mutant reveal cell-extrinsic determinants of neuronal morphology. J. Neurosci. 13, 4254–4271.

Hosono, R., 1978. Sterilization and growth inhibition of *Caenorhabditis elegans* by 5-fluorodeoxyuridine. Exp. Gerontol. 13, 369–374.

Hutter, H., Vogel, B.E., Plenefisch, J.D., Norris, C.R., Proenca, R.B., Spieth, J., Guo, C., Mastwal, S., Zhu, X., Scheel, J., Hedgecock, E.M., 2000. Conservation and novelty in the evolution of cell adhesion and extracellular matrix genes. Science 287, 989–994.

Kamath, R.S., Martinez-Campos, M., Zipperlen, P., Fraser, A.G., Ahringer, J., 2001. Effectiveness of specific RNA-mediated interference through ingested double-stranded RNA in *Caenorhabditis elegans*. Genome Biol. 2, RESEARCH0002.

Kaneko-Goto, T., Yoshihara, S., Miyazaki, H., Yoshihara, Y., 2008. BIG-2 mediates olfactory axon convergence to target glomeruli. Neuron 57, 834–846.

Karagogeos, D., 2003. Neural GPI-anchored cell adhesion molecules. Front. Biosci. 8, s1304–s1320.

Katidou, M., Vidaki, M., Strigini, M., Karagogeos, D., 2008. The immunoglobulin superfamily of neuronal cell adhesion molecules: lessons from animal models and correlation with human disease. Biotechnol. J. 3, 1564–1580.

Killeen, M.T., Sybingco, S.S., 2008. Netrin, Slit and Wnt receptors allow axons to choose the axis of migration. Dev. Biol. 323, 143–151.

Kolodkin, A.L., Tessier-Lavigne, M., Mechanisms and molecules of neuronal wiring: a primer. Cold Spring Harb. Perspect. Biol. 3.

Kyriakopoulou, K., de Diego, I., Wassef, M., Karagogeos, D., 2002. A combination of chain and neurophilic migration involving the adhesion molecule TAG-1 in the caudal medulla. Development 129, 287–296.

Levy-Strumpf, N., Culotti, J.G., 2007. VAB-8, UNC-73 and MIG-2 regulate axon polarity and cell migration functions of UNC-40 in *C. elegans*. Nat. Neurosci. 10, 161–168.

Maness, P.F., Schachner, M., 2007. Neural recognition molecules of the immunoglobulin superfamily: signaling transducers of axon guidance and neuronal migration. Nat. Neurosci. 10, 19–26.

Martinez-Lopez, M.J., Alcantara, S., Mascaro, C., Perez-Branguli, F., Ruiz-Lozano, P., Maes, T., Soriano, E., Buesa, C., 2005. Mouse neuron navigator 1, a novel microtubule-associated protein involved in neuronal migration. Mol. Cell. Neurosci. 28, 599–612.

Mayor, S., Riezman, H., 2004. Sorting GPI-anchored proteins. Nat. Rev. Mol. Cell Biol. 5, 110–120.

McIntire, S.L., Jorgensen, E., Horvitz, H.R., 1993. Genes required for GABA function in *Caenorhabditis elegans*. Nature 364, 334–337.

Powell, P.A., Wesley, C., Spencer, S., Cagan, R.L., 2001. Scabrous complexes with Notch to mediate boundary formation. Nature 409, 626–630.

Rougon, G., Hobert, O., 2003. New insights into the diversity and function of neuronal immunoglobulin superfamily molecules. Annu. Rev. Neurosci. 26, 207–238.

Roy, P.J., Zheng, H., Warren, C.E., Culotti, J.G., 2000. mab-20 encodes Semaphorin-2a and is required to prevent ectopic cell contacts during epidermal morphogenesis in *Caenorhabditis elegans*. Development 127, 755–767.

Rugarli, E.I., Di Schiavi, E., Hilliard, M.A., Arbucci, S., Ghezzi, C., Facciolli, A., Coppola, G., Ballabio, A., Bazzicalupo, P., 2002. The Kallmann syndrome gene homolog in *C. elegans* is involved in epidermal morphogenesis and neurite branching. Development 129, 1283–1294.

Sasakura, H., Inada, H., Kuhara, A., Fusaoka, E., Takemoto, D., Takeuchi, K., Mori, I., 2005. Maintenance of neuronal positions in organized ganglia by SAX-7, a *Caenorhabditis elegans* homologue of L1. EMBO J. 24, 1477–1488.

Schmidt, K.L., Marcus-Gueret, N., Adeleye, A., Webber, J., Baillie, D., Stringham, E.G., 2009. The cell migration molecule UNC-53/NAV2 is linked to the ARP2/3 complex by ABI-1. Development 136, 563–574.

Schmitz, C., Kinge, P., Hutter, H., 2007. Axon guidance genes identified in a large-scale RNAi screen using the RNAi-hypersensitive *Caenorhabditis elegans* strain nre-1(hd20) lin-15b(hd126). Proc. Nat. Acad. Sci. U.S.A. 104, 834–839.

Schwarz, V., Pan, J., Voltmer-Irsch, S., Hutter, H., 2009. IgCAMs redundantly control axon navigation in *Caenorhabditis elegans*. Neural Dev. 4, 13.

Shen, K., Fetter, R.D., Bargmann, C.I., 2004. Synaptic specificity is generated by the synaptic guidepost protein SYG-2 and its receptor, SYG-1. Cell 116, 869–881.

Shimoda, Y., Watanabe, K., 2009. Contactins: emerging key roles in the development and function of the nervous system. Cell Adhesion Migr. 3, 64–70.

Stringham, E., Pujol, N., Vandekerckhove, J., Bogaert, T., 2002. unc-53 controls longitudinal migration in *C. elegans*. Development 129, 3367–3379.

Stringham, E.G., Schmidt, K.L., 2009. Navigating the cell: UNC-53 and the navigators, a family of cytoskeletal regulators with multiple roles in cell migration, outgrowth and trafficking. Cell Adhesion Migr., 3.

Timmons, L., Fire, A., 1998. Specific interference by ingested dsRNA. Nature 395, 854.

Trent, C., Tsuing, N., Horvitz, H.R., 1983. Egg-laying defective mutants of the nematode *Caenorhabditis elegans*. Genetics 104, 619–647.

Tsibidis, G.D., Tavernarakis, N., 2007. Nemo: a computational tool for analyzing nematode locomotion. BMC Neurosci. 8, 86.

Voglis, G., Tavernarakis, N., 2008. A synaptic DEG/ENaC ion channel mediates learning in *C. elegans* by facilitating dopamine signalling. EMBO J. 27, 3288–3299.

Von Stetina, S.E., Treinin, M., Miller 3rd, D.M., 2006. The motor circuit. Int. Rev. Neurobiol. 69, 125–167.

Wang, X., Zhang, W., Cheever, T., Schwarz, V., Opperman, K., Hutter, H., Koepp, D., Chen, L., 2008. The *C. elegans* L1CAM homologue LAD-2 functions as a coreceptor in MAB-20/Sema2 mediated axon guidance. J. Cell Biol. 180, 233–246.

Watari-Goshima, N., Ogura, K., Wolf, F.W., Goshima, Y., Garriga, G., 2007. *C. elegans* VAB-8 and UNC-73 regulate the SAX-3 receptor to direct cell and growth-cone migrations. Nat. Neurosci. 10, 169–176.

Weinstein, B.M., 2005. Vessels and nerves: marching to the same tune. Cell 120, 299–302.

White, J.G., Southgate, E., Thomson, J.N., Brenner, S., 1976. The structure of the ventral nerve cord of *Caenorhabditis elegans*. Philos. Trans. R. Soc. London, Ser. B Biol. Sci. 275, 327–348.

White, J.G., Southgate, E., Thomson, J.N., Brenner, S., 1986. The structure of the nervous system of the nematode *Caenorhabditis elegans*. Philos. Trans. R. Soc. London, Ser. B 314, 1–340.

Yoshihara, Y., Kawasaki, M., Tamada, A., Nagata, S., Kagamiyama, H., Mori, K., 1995. Overlapping and differential expression of BIG-2, BIG-1, TAG-1, and F3: four members of an axon-associated cell adhesion molecule subgroup of the immunoglobulin superfamily. J. Neurobiol. 28, 51–69.